BMC Neuroscience

RESEARCH Open Access

Role of the sympathetic nervous system in cancer-associated cachexia and tumor progression in tumor-bearing BALB/c mice

Isaias Gutierrez-Leal[1], Diana Caballero-Hernández[1*], Alonso A. Orozco-Flores[1], Ricardo Gomez-Flores[1], Deyanira Quistián-Martínez[2], Patricia Tamez-Guerra[1], Reyes Tamez-Guerra[1] and Cristina Rodríguez-Padilla[1]

Abstract

Background Adipose and muscle tissue wasting outlines the cachectic process during tumor progression. The sympathetic nervous system (SNS) is known to promote tumor progression and research suggests that it might also contribute to cancer-associated cachexia (CAC) energetic expenditure through fat wasting.

Methods We sympathectomized L5178Y-R tumor-bearing male BALB/c mice by intraperitoneally administering 6-hydroxydopamine to evaluate morphometric, inflammatory, and molecular indicators of CAC and tumor progression.

Results Tumor burden was associated with cachexia indicators, including a 10.5% body mass index (BMI) decrease, 40.19% interscapular, 54% inguinal, and 37.17% visceral adipose tissue loss, a 12% food intake decrease, and significant ($p=0.038$ and $p=0.0037$) increases in the plasmatic inflammatory cytokines IL-6 and IFN-γ respectively. Sympathectomy of tumor-bearing mice was associated with attenuated BMI and visceral adipose tissue loss, decreased interscapular *Ucp-1* gene expression to basal levels, and 2.6-fold reduction in *Mmp-9* relative gene expression, as compared with the unsympathectomized mice control group.

Conclusion The SNS contributes to CAC-associated morphometric and adipose tissue alterations and promotes tumor progression in a murine model.

Keywords Cancer cachexia, Lymphoma, Sympathetic nervous system, Adrenergic system, Inflammation, Sympathectomy

*Correspondence:
Diana Caballero-Hernández
diana.caballerohr@uanl.edu.mx
[1]Facultad de Ciencias Biológicas, Laboratorio de Inmunología y Virología, Universidad Autónoma de Nuevo León, Apartado postal 46 F, San Nicolás de los Garza, NL 66451, Mexico
[2]Facultad de Ciencias Biológicas, Departamento de Botánica, Universidad Autónoma de Nuevo León, San Nicolás de los Garza, NL 66451, Mexico

Introduction

Cancer-associated cachexia (CAC) is a wasting syndrome characterized by weight loss, and muscle and adipose tissue depletion that is not reversed by a standard nutritional approach. Cancer cachexia profoundly affects quality of life of patients and may interfere with their ability to cope with anticancer treatments [1]. It is also defined as an inflammatory state characterized by elevated levels of pro-inflammatory cytokines in serum [2]. Cancer cachexia is prevalent among various cancers, including solid tumors and hematological cancers such as lymphomas, contributing to patient outcomes, including survival [3, 4]. Although adipose tissue wasting is attributed to many factors, the mechanisms underlying CAC-related white adipose tissue lipolysis and brown fat browning remain to be elucidated. In this regard, the sympathetic nervous system (SNS) is known to regulate adipose tissue deposits through beta-adrenergic receptor activation by norepinephrine (NE). Previous studies have highlighted the role of interscapular adipose tissue browning and the role of β-3 adrenergic receptors in CAC. Petruzelli [5] et al. demonstrated that adipose tissue browning was an early event in CAC and that the β-3 adrenergic blocker SR 59230A attenuated adipose tissue browning in a melanoma tumor model. In addition, Jin [6] et al. used a chemical variant of L-748,337, a β-3 adrenergic antagonist, and observed a decrease in serum glycerol in C26 tumor-bearing mice. Furthermore, studies have shown that NE promotes tumor progression through most hallmarks of cancer by adrenergic β-1, 2 receptor activation [7]. We have previously demonstrated changes in cachexia-associated indicators, including adipose tissue depletion, reduced food intake, and morphological alterations in L5178Y-R lymphoma-bearing BALB/c mice, and have consistently observed increased plasmatic NE levels in this model, suggesting that tumors may act as a stressor and activate the SNS pathway during cancer progression [8]. Up to 35% of non-Hodgkin lymphoma (NHL) patients will develop cachexia, and its progression is assessed using their weight and BMI as markers [9]. Despite studies on sympathectomy or beta-blockers treatment in lymphoma patients are scarce, it has been observed that beta-blockers prevent cardiotoxicity from chemotherapy in NHL patients [10]. Although the mechanisms remain to be elucidated, beta-blockers may be targeting abnormal lipid metabolism, a feature of cancer that has been found associated with resistance to chemotherapy [11]. The ectopic lymphoma model used in our study displays sufficient cachectic features, making it useful for exploring the contribution of the SNS to cancer cachexia. Regardless of the precise mechanisms mediating tumor-induced activation of the SNS, studies in lymphoma patients have found autonomic dysfunction that disappears in cured patients [12]. This autonomic dysfunction might lead to a hyperactive SNS with increased NE secretion to the bloodstream [13]. Furthermore, the dense sympathetic innervation in the mouse hind limb muscles [14], provides a microenvironment where the tumor mass may interact with sympathetic nerves and a useful model to determine the potential of a tumor mass to activate the SNS. It also shows its relevance for tumor-associated syndromes such as cachexia.

Supported by previous observations of elevated plasmatic NE and cachectic features in this tumor model, our aim was to explore the SNS contribution to adipose tissue wasting and cancer progression in the L5178Y-R murine model. To achieve this, we performed peripheral sympathectomy, using the neurotoxin 6-hydroxydopamine (6-OHDA), which specifically targets sympathetic innervation and does not cross the blood-brain barrier. We used a transplantable tumor model, subcutaneously implanted on the mouse hind limb. To assess the extent of SNS contribution to tumor progression and cachexia, we evaluated morphological parameters of interscapular adipose tissue, plasma inflammation cytokines, and the composition of brown, beige, and white adipose tissue deposits, as well as tumor progression indicators.

Materials & methods

Animals

We used 10- to 12-week-old male BALB/c mice, obtained from the animal facility at Facultad de Ciencias Biológicas, Universidad Autónoma de Nuevo León (UANL), México. Mice were kept in microventilated cages with access to food and water *ad libitum*, under a 12-hour light/dark cycle, at a controlled temperature of 22 °C and 45% relative humidity. Cages were enriched with cardboard tubes for mouse recreation. All experiments complied with Mexican regulation NOM-062-ZOO-1999 and were approved by the UANL Research Ethics and Animal Welfare Committee (CEIBA-2021-003). Mice were randomly distributed into the tumor-free ($n=6$), tumor free+sympathectomy ($n=6$), tumor ($n=6$), and tumor+sympathectomy ($n=5$) groups, which were kept in cages one week before sympathectomy for acclimatization. Researchers were aware of the identity of the animal groups and their respective treatments throughout the experiments.

Tumor model

For tumor experiments, the murine lymphoma L5178Y-R cell line (female mouse DBA/2 lymphoma) was purchased from The American Type Culture Collection (Rockville, MD, USA) and maintained in culture flasks with RPMI 1640 medium supplemented with 10% fetal bovine serum (FBS), 1% L-glutamine, and 0.5% penicillin-streptomycin solution from Sigma-Aldrich (St. Louis,

MO, USA) at 37 °C and 5% CO_2 in air, in a humidified atmosphere.

Sympathectomy and tumor implantation

Chemical sympathectomy was performed by intraperitoneal injection of two doses of 100 mg/kg (body weight) 6-OHDA (Sigma-Aldrich) on two consecutive days. Sympathectomy was considered complete four days after the initial dose, showing reduced NE in the spleen as previously reported [15]. Tumors were implanted six days after the second dose of 6-OHDA. L5178Y-R cells were subcutaneously implanted in the mouse posterior right hindlimb muscles by injecting 2×10^6 cells in 100 µL of phosphate-buffered saline; tumor-free animals received only the vehicle.

To adhere to humane endpoint criteria, mice welfare was monitored at least twice daily, following internal guidelines. Humane endpoints included tumor dimensions exceeding 20 mm in any direction, signs of pain or sickness behaviors, abdominal distention, a low body score condition, or other indications of suffering.

Body weight and body mass index calculation

Mouse body weight was measured every second day using a digital scale and final body weight was corrected by subtracting the excised tumor mass weight. Mice body mass index (BMI), also known as the Lee index, was calculated at the endpoint, as the product of dividing the corrected body weight between the square of the nose-anus length [16].

Daily and total food and water intake

Food and water intake were measured at days 9, 11, 13, 15, 17 and 19. A fixed amount of food and water were placed in the cage and two days later the remaining amounts were calculated, individual intake by time point was calculated as the difference between the initial and remaining amounts of food and water, divided by the number of mice by cage. For statistical analysis, intake by time points were compared between experimental groups. Food was weighed using a digital scale and water was measured using a 100 mL graduated cylinder. To prevent social isolation stress, the animals of each experimental group were kept together in a cage.

Tumor progression

Tumor volume was determined by measuring the length and width of the tumor mass with a digital caliper (Fischer Scientific, Hampton, NH, USA) every third day. To calculate tumor volume, the following formula was used: tumor volume (mm^3) = 1/2 (length x $width^2$). After mice were euthanized, tumors were excised and weighed on an analytical scale.

Mmp-2, *Mmp-9*, and *Ucp-1* gene expression

Total RNA was extracted from the excised tumors, using the QIAzol lysis reagent (Qiagen Sciences, Frederick, MD, USA) and following manufacturer´s instructions. RNA concentration was quantified to ensure DNA purity. The A260/280 ratio was assessed using a NanoDrop 2000 (Thermo Fisher Scientific, Waltman, MA, USA). Two micrograms of RNA were retrotranscribed to complementary DNA, using the High-Capacity cDNA Reverse Transcription Kit (Thermo Fisher Scientific). The relative expression of *Mmp-2* and *Mmp-9* was determined using the TaqMan probes for *Mmp-2* and *Mmp-9* (assay numbers MM00439498_M1 and MM00442991_M1 respectively), and *Gapdh* as housekeeping gene (assay number Mm99999915_g1). For Ucp-1 gene expression analysis, primers were designed for mouse *Ucp-1* as follows: forward 5´ AGT ACC CAA GCG TAC CAA GC-3´ and reverse 5´ TCG TGG TCT CCC AGC ATA GA-3´ for a 248 amplicon. As an endogenous gene, beta-actin primers were designed as follows: forward 5´ TGA GCT GCG TTT TAC AC CCT-3´ and reverse 5´GCC TTC ACC GTT CCA GTT TTT-3´ for a 198 pb amplicon. All primers were purchased from Integrated DNA Technologies (Coralville, IA, USA). Real-time PCR reactions were set following the GoTaq qPCR Master Mix (Promega Madison, WI, USA) instructions. Duplicated reactions were run in a 7500 Real-Time PCR System (Applied Biosystems, Waltham, MA, USA). Melting curve assay was performed to ensure primer specificity. Data were analyzed with the 2(−ΔΔCt) formula, using the Livak method [17].

Interscapular adipose tissue histological analysis

Excised interscapular adipose tissue was fixed in 10% formaldehyde for 72 h, washed in PBS, and stored in 70% ethanol at 4 °C, until use. Samples were embedded in paraffin and stained by the hematoxylin and eosin method. Histological preparations were produced and digitized images were obtained by a camera under a 40X/0.65 objective microscope (Carl Zeiss, Göttingen, Germany). Images were analyzed (three photographs per tissue) by the Image J software (NIH ImageJ; NIH, Bethesda, MD, USA). The Adiposoft plugin was used to calculate the cellular area [18].

Sample collection

Animals were anesthetized with an intraperitoneal dose administration of 30 mg/kg pentobarbital, followed by cardiac puncture with a one-milliliter syringe and a 27 G x 13 mm Luer Lock needle with traces of EDTA. Blood was collected in a 1.5 mL microtube, centrifuged at 5000 rpm for 10 min, and stored at -80 °C. After blood collection, anesthetized animals were euthanized by cervical dislocation. Tumor, adipose tissue, and the gastrocnemius muscle were excised and stored at -80 °C.

Plasmatic cytokines

Plasma levels of IL-6, IL-10, IL-12p70, IFN-γ, TNF-α, and MCP-1 were quantified with the Cytometric Bead Array Mouse inflammation kit from BD Biosciences (San Jose, CA, USA), following the manufacturer´s instructions. Samples were processed in an Accuri 6 flow cytometer (BD Biosciences, Ann Arbor, MI, USA) and data were analyzed with the FCAP Array Software V 3.0 (Soft Flow Hungary, Ltd., Pécs, Hungary).

Statistical analysis

Normality distribution was determined by the Kolmogorov-Smirnov test. Parametric determinations were evaluated using a one-way ANOVA, followed by planned multiple comparisons with the Bonferroni correction to compare tumor-free vs. tumor-free+sympathectomy, tumor free vs. tumor, and tumor vs. tumor+sympathectomy. For non-parametric evaluations, we applied the Kruskal-Wallis test, followed by Dunn's planned comparisons. For body weight analysis, a one-way repeated measures ANOVA was performed with between-groups comparison. For metalloproteinase gene expression, each gene was independently compared with the control by the Dunn test.

Results

Body weight

We observed a significant decrease in body weight in sympathectomized mice 24 h after the intervention. The sympathectomized groups decreased 17.3% (tumor-free+sympathectomy) and 12.36% (tumor+sympathectomy) their body weight following sympathectomy on days 3 ($p=0.011$) and 5 ($p=0.03$), a weight that was recovered by day 7 (Fig. 1a). We did not observe significant changes in body weight after tumor implantation.

Body mass index (BMI)

To calculate the BMI, excised tumors were subtracted for weight correction. We showed a significant ($p=0.033$) 10.5% decrease in BMI associated with tumor burden, observing a BMI of 0.38 g/cm^2 compared with a 0.42 g/cm^2 BMI in the tumor-free group. Recovery of the BMI was observed in the sympathectomy+tumor group with a BMI of 0.43 g/cm^2 (Fig. 1b).

Food and water intake

After sympathectomy, both groups showed decreasing food and water intake, which was recovered by day 7. Since tumor implantation was performed on day 9, we calculated the total food intake starting from day 9. All groups showed a food intake ranging from 10.5 to 11.1 g per time point. The tumor and tumor+sympathectomy groups' food intake was below ten grams per time point, at day 15. Animals in the tumor group consumed 9.58 g per time point, as compared with 11.58 g for animals in the tumor-free group as shown in Tables 1 and 2 (supplementary material). We also found a significant ($p=0.03$) reduction in tumor-associated food intake, from 11.22 to 9.82 g (12% reduction), as compared with the tumor-free group (Fig. 2a). We did not observe a significant difference in water intake between the groups (Fig. 2b).

Body fat and muscle content

Significant ($p=0.001$, $p=0.0007$, and $p=0.0085$) body fat decreases were observed in the tumor-bearing group for interscapular (40.19% reduction), inguinal (54% reduction), and visceral fat (37.17% reduction) body deposits, as compared with tumor-free mice. Furthermore, visceral sympathectomy significantly ($p=0.05$) attenuated visceral fat loss in animals of the tumor+sympathectomy group, with an increase in visceral fat, as compared with the tumor-bearing group. We also observed a significant ($p=0.0097$) increase in interscapular adipose tissue percentage in tumor-free sympathectomized animals,

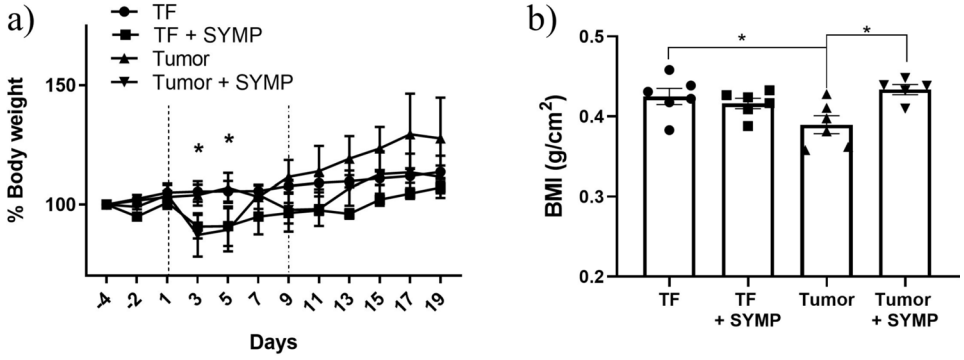

Fig. 1 Body weight and BMI in sympathectomized and tumor-bearing mice. Sympathectomy (SYMP) was performed in tumor-bearing and tumor-free (TF) mice (**a**) Body weight gain is expressed as a percentage relative to body weight at day −4. Dotted lines mark the day of sympathectomy and tumor implantation, respectively and (**b**) tumor weight was subtracted from body weight for BMI calculations. Values are expressed as the mean ± SEM of 5–6 mice from a representative experiment. *$p \leq 0.05$

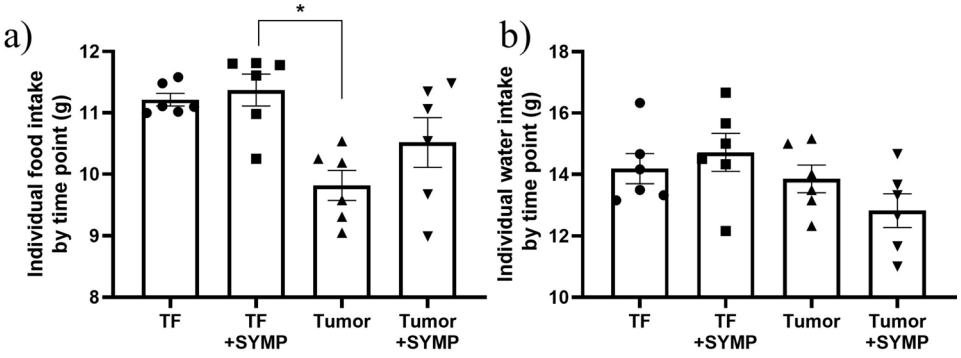

Fig. 2 Food and water intake. Food (**a**) and water (**b**) intake were measured at days 9, 11, 13, 15, 17 and 19 during the experiment for all experimental groups. A fixed amount of food and water were placed in the cage and two days later the remaining amounts were calculated. Individual intake by time point was calculated as the difference between the initial and remaining amounts of food and water in each cage, divided by the number of mice housed in the cage. Values are expressed as the mean ± SEM of 6 time points for each cage housing 6 mice from a representative experiment. *$p \leq 0.05$

as compared with animals of the tumor-free group ($p=0.0097$), indicating attenuation of basal thermogenesis (Fig. 3a). No statistical differences were observed in gastrocnemius or muscle content among the groups (Fig. 3b).

Adipocyte size and Ucp-1 gene expression in interscapular brown adipose (iBAT) tissue

Adipocyte area size in pixels and adipose tissue content significantly ($p=0.003$) increased in the tumor-free + sympathectomy group, as compared with the tumor-free group. We did not observe statistical differences in adipocyte size in the rest of the comparisons (Fig. 3c). In addition, a 6.2-fold significant ($p=0.03$) increase in *Ucp-1* gene expression in the tumor group was observed. Furthermore, iBAT *Ucp-1* relative gene expression was recovered ($p=0.01$) to a 1.06-fold in tumor-bearing sympathectomized mice (Fig. 3d).

Pro-inflammatory cytokines

Plasmatic levels of IL-6 and IFN-γ significantly ($p=0.038$ and $p=0.0037$, respectively) increased in tumor-bearing mice, as compared with the tumor-free control group. We did not observe significant changes in TNF-α, IL-10, MCP-1, and IL-12p70 cytokine levels (Fig. 4).

Tumor volume, tumor final weight, and *Mmp-2*, *Mmp-9* gene expression

We did not show significant differences in final tumor volume and weight between the sympathectomized and non-sympathectomized groups (Fig. 5a and b). In the tumor + sympathectomy group, one mouse did not grow a tumor and was discarded. As for molecular indicators of tumor progression, tumor *Mmp-2* gene expression was unaffected by sympathectomy, whereas tumor *Mmp-9* gene expression had a significant ($p=0.025$) 2.267-fold decrease (Fig. 5c).

Discussion

Cancer-associated cachexia is a wasting syndrome characterized by weight loss and muscle and adipose tissue depletion [1]. In the present study, we used sympathectomy in a mouse model of lymphoma to investigate the role of the SNS in the development of cachexia. We found that sympathectomy reversed a decrease in BMI associated with tumor burden. The SNS is known to regulate fat content in white adipose tissue deposits through lipolysis and thermogenesis activation in brown adipose tissue [19]. In our murine model, adipose tissue wasting was evident in three different deposits but sympathectomy did not revert this effect in the interscapular or inguinal fat deposit. We observed that visceral fat depletion was attenuated in sympathectomized tumor-bearing mice, which may partially explain BMI recovery. Since there was no statistical difference in the gastrocnemius muscle or heart weight, our cachexia model may be characterized by adipose tissue but not muscle depletion. Although we measured the three major adipose tissue deposits, a more sensitive technique such as MRI may provide us with a more precise evaluation of changes in adipose tissue deposits and skeletal muscles. In addition, the L5178Y-R tumor takes approximately 10 d to reach the humane endpoint based on tumor volume, limiting the time frame for observation. We also observed that the weight of interscapular adipose tissue, a major deposit of BAT in mice, was greater in the sympathectomy group among the tumor-free groups. This might be explained by the effect of baseline thermogenesis required to regulate the mouse body temperature under laboratory conditions since mouse thermoneutrality is closer to 32 °C and has been reported to increase up to 37 °C in tumor-bearing mice [20]. In contrast, sympathectomy did not prevent iBAT depletion in tumor-bearing mice, which suggests that other lipolytic factors, antitumor systemic cytokines, or the tumor secretome, might also be responsible for iBAT depletion in tumor-bearing mice.

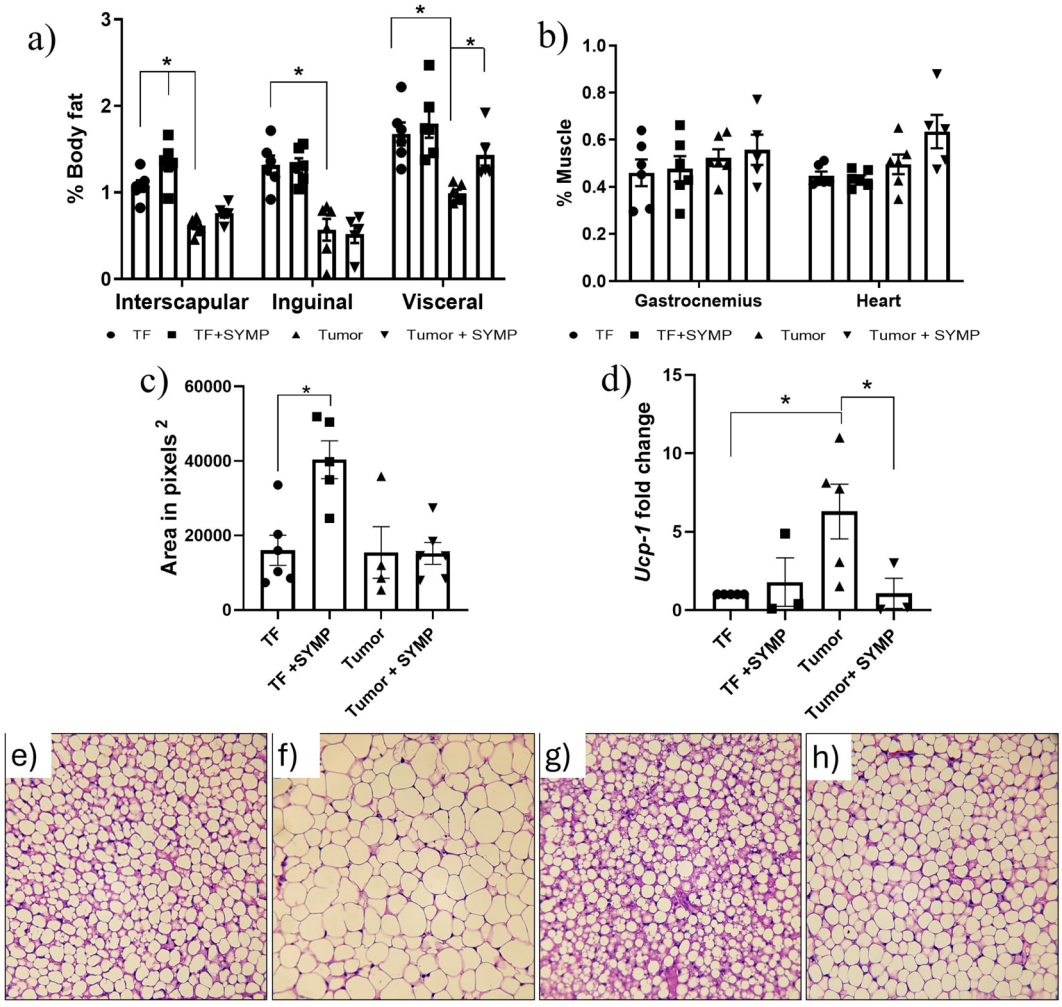

Fig. 3 Adipose and muscle wasting indicators. Adipose tissue content, adipocyte size and *Ucp1* transcriptional expression were assessed in the tumor-free (TF), tumor-bearing and sympathectomized (SYMP) groups. (**a**) Body fat percentage in different adipose tissue deposits. (**b**) Muscle body percentage in gastrocnemius and heart. (**c**) Adipocyte area size in interscapular adipose tissue (**d**) *Ucp-1* relative expression in interscapular adipose tissue. Representative images of histological preparations of interscapular adipose tissue in (**e**) tumor-free, (**f**) tumor-free + sympathectomy, (**g**) tumor-bearing, and (**h**) tumor-bearing + sympathectomy groups. Adipocyte area size was calculated using the Adiposoft plugin from image J. Data are expressed as the mean ± SEM of 5–6 mouse and 3–6 for *Ucp-1* analysis from a representative experiment. *$p \leq 0.05$

Relative gene expression of *Ucp-1*, a molecular marker for thermogenesis, also increased in tumor-bearing animals, returning to basal levels in the sympathectomized mice. Ucp-1, also known as thermogenin, is involved in thermoregulation. In mice, iBAT is upregulated by the SNS, mostly through β-3 adrenergic receptors [21]. The immune antitumor response may potentially mediate cachexia features in the L5178Y-R model. In this regard, we measured a set of pro-inflammatory cytokines in plasma and observed increased levels of cachexia-associated cytokines. Particularly, IL-6 and IFN-γ plasmatic level increases were associated with tumor burden but remained elevated regardless of sympathectomy. In this regard, IL-6 also has been shown to induce fat wasting and thermogenesis. In a study in the BALB/c mice colon 26 cancer model, both inguinal fat wasting and iBAT browning were observed, changes that were prevented by anti-IL-6 antibodies [22]. This finding, along with the fact that iBAT activation is inhibited by sympathectomy only in the tumor-free group, suggests that iBAT activation in our tumor model might be driven by other tumor-induced factors, such as IL-6. Han [22] et al. also observed inguinal fat depletion associated with tumor burden and wasting attenuation due to anti-IL-6 treatment in the C-26 colorectal cancer murine model. In the murine lymphoma model, we also observed inguinal fat wasting that was not affected by sympathectomy. This might be explained by differences in tumor type and tumor implantation site. In our model, the tumor is located closer to the inguinal deposit. In addition, interscapular, inguinal, and visceral fat not only differ by their location but also in their functions. Whereas the main

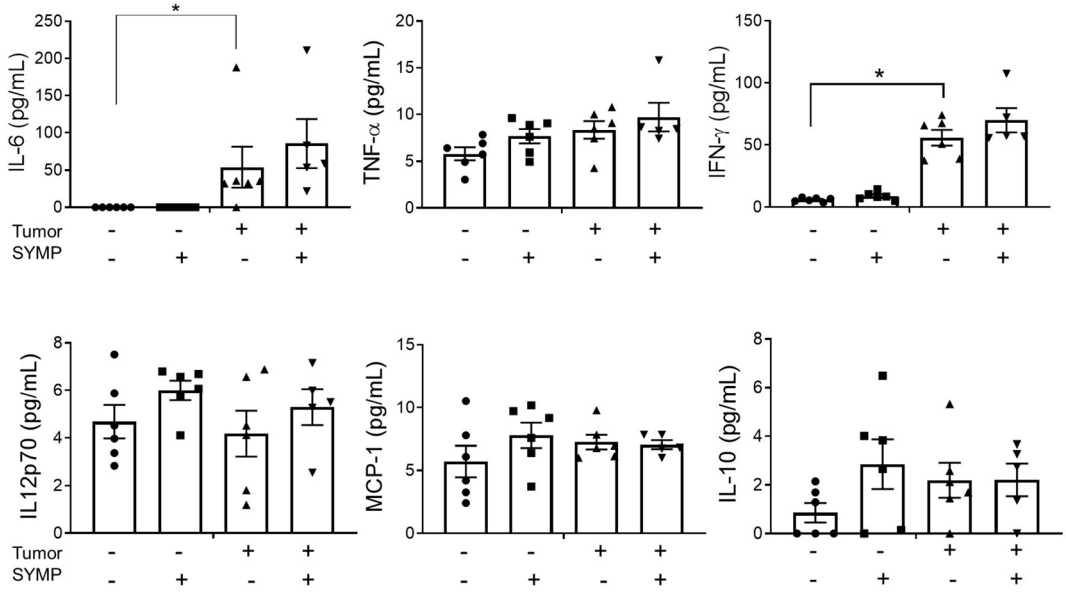

Fig. 4 Inflammatory cytokines in tumor-bearing and sympathectomized mice. Plasmatic cytokines were quantified by flow cytometry in intact and sympathectomized (SYMP) tumor-free and tumor-bearing mice. Data are expressed as the mean ± SEM of 5–6 mice from a representative experiment. *$p \leq 0.05$

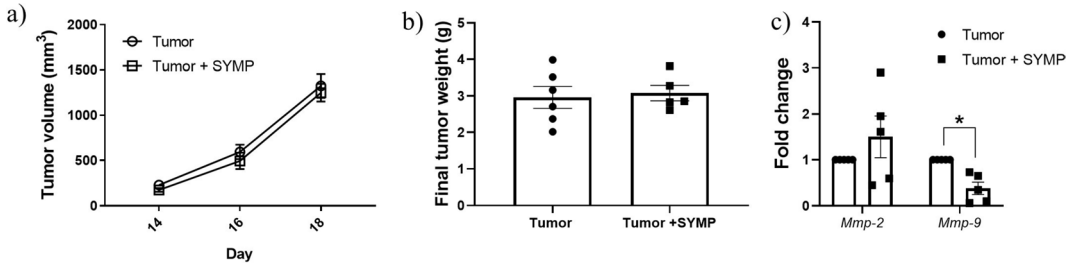

Fig. 5 Tumor progression indicators. (**a**) Tumor volume and (**b**) tumor final weights in intact and sympathectomized (SYMP) mice. (**c**) Relative gene expression of the metalloproteinases Mmp-2 and Mmp-9 in tumor samples. Data are expressed as the mean ± SEM of 5–6 mice from a representative experiment. *$p \leq 0.05$

role of the interscapular adipose tissue is thermogenesis, inguinal and visceral white fat mainly function as energy storage [23]. We also showed in tumor-bearing mice an increase in IFN-γ, a known inflammatory cytokine that is associated with cachexia in many types of cancers [24]. IFN-γ has been shown to participate in muscle wasting and body weight loss in mice bearing the Lewis lung carcinoma [25]. In addition, IFN-γ expression has been observed in the mesenteric adipose tissue in the cachectic Walker 256 rat model. Furthermore, an increase in *Ifngr1*, the IFN-γ receptor, has been associated with cachectic features, including weight loss and reduced food intake in Wistar rats [26]. In addition to IL-6, IFN-γ might also contribute to the morphometric alterations observed in iBAT and adipose tissue wasting in inguinal adipose tissue in our model. Regarding changes in eating behavior, anorexia is another important feature of CAC. We observed a 12% decrease in food intake in the tumor-bearing groups. In a study in C57BL/6 mice bearing the cachectic CHX207 fibrosarcoma a 15% reduction in food intake was observed but no differences in water intake were found [27], similar to the findings in our study. In addition, inflammatory cytokines such as IL-6 have been shown to contribute to inflammation-induced anorexia in the hypothalamus [28]. The SNS is also involved in food intake regulation, specifically through β-3 adrenergic receptors in the central nervous system [29]. However, sympathectomy alone did not exert a statistically significant effect on food intake, suggesting that IL-6 or other factors might be responsible for the anorexic effects observed in this particular tumor model. Regarding tumor progression, it is well known that the SNS has a promoting role by directly affecting all hallmarks of cancer [7]. In our lymphoma cancer model, we did not observe changes in tumor volume or tumor final weights in the sympathectomized groups. This contrasts with the findings of Nissen [30] et al., who reported in a mouse model of B-cell lymphoma, that treatment with the

beta-adrenergic agonist isoprenaline, promoted tumor development, and suppressed proliferation, IFN-γ production, and cytolytic activity by antigen-specific T cells. Conflicting findings have also been reported for the mouse melanoma B16 model, where sympathectomy has been associated either with increasing tumor weight and extended survival [6] or decreasing tumor weight [21]. Horvathova et al. also showed that expression of the *Bcl-2* and *Caspase-3* genes, which are related to apoptosis, increased after sympathectomy, providing a potential mechanism for the antitumoral effect observed [21].

Although no reduction in tumor size was found for sympathectomized tumor-bearing mice, we analyzed the relative gene expression of the metalloproteases Mmp-2 and Mmp-9 in tumors, aiming to identify early changes potentially relevant for tumor progression at the molecular level. We found that after sympathectomy the expression of *Mmp-2* was unaffected, whereas expression of *Mmp-9* decreased. Metalloproteins are relevant for several aspects of cancer progression, including invasion, migration, and inflammation [31]. Previous reports in nude male Foxn mice bearing prostate cancer DU145 tumor cells have shown that NE treatment did not influence tumor volume but increased Mmp-2 and Mmp-9 protein expression, according to immunohistochemistry analysis [32] molecular markers for tumor properties such as invasiveness and metastasis may be useful for assessing tumor progression in addition to measuring tumor size. Interestingly, increasing Mmp-9 expression in cardiac and skeletal muscle has also been reported for cancer cachexia in the C26 adenocarcinoma model [33], suggesting its potential role in muscle changes associated to cachexia.

Our study has an important limitation. Our findings were obtained in a subcutaneous instead of an orthotopic tumor model of cancer. Although the subcutaneous L5178Y-R lymphoma shows distinct cachexia features, allowing us to explore the contribution of the SNS to this syndrome, orthotopic models are considered to better replicate the tumor microenvironment, thus becoming clinically more relevant than subcutaneous models.

Conclusions

In a mouse model of lymphoma that resembles cachexia features such as fat wasting, brown adipose tissue thermogenesis, decreasing BMI, and food intake plus an elevation in plasmatic IL-6 and IFN-γ, the SNS contributes to the cachectic phenotype, promoting white but not brown adipose tissue wasting and upregulating the expression of genes relevant for tumor invasiveness during cancer progression.

Supplementary Information

The online version contains supplementary material available at https://doi.org/10.1186/s12868-024-00887-8.

Supplementary Material 1

Supplementary Material 2

Supplementary Material 3

Acknowledgements

The authors want to thank M.Sc. Alejandra Arreola-Triana for manuscript suggestions.

Author contributions

I.G.L., D.C.H., R.T.G. and C.R.P.: Conceived and designed the experiments; I.G.L. wrote the original draft, reviewed and edited; I.G.L., A.A.O.F. and D.Q.M. Performed experiments and prepared figures. D.C.H., R.G.F., P.T.G. analyzed data, reviewed and edited manuscript. All authors reviewed the results and approved the final version of the manuscript.

Funding

I.G.L. received a fellowship grant from CONAHCYT with ID 966540. D.C.H. was awarded a PAICYT grant with ID CN1182-20 from Universidad Autónoma de Nuevo León.

Data availability

Data is available as supplementary material.

Declarations

Ethics approval and consent to participate

All experiments with animals complied with Mexican regulation NOM-062-ZOO-1999 and were approved by the UANL Research Ethics and Animal Welfare Committee (CEIBA-2021-003).

Consent for publication

Not applicable.

Competing interests

The authors declare no competing interests.

Received: 18 April 2024 / Accepted: 14 August 2024
Published online: 22 August 2024

References

1. Fearon K, Strasser F, Anker SD, Bosaeus I, Bruera E, Fainsinger RL, et al. Definition and classification of cancer cachexia: an international consensus. Lancet Oncol. 2011;12:489–95. https://doi.org/10.1016/S1470-2045(10)70218-7.
2. Riccardi DMDR, das Neves RX, de Matos-Neto EM, Camargo RG, Lima JDCC, Radloff K, et al. Plasma lipid Profile and systemic inflammation in patients with Cancer Cachexia. Front Nutr. 2020;7:4. https://doi.org/10.3389/fnut.2020.00004.
3. Letilovic T, Perkov S, Mestric ZF, Vrhovac R. Differences in routine laboratory parameters related to cachexia between patients with hematological diseases and patients with solid tumors or heart failure - is there only one cachexia? Nutr J. 2013;12:6. https://doi.org/10.1186/1475-2891-12-6.
4. Karmali R, Alrifai T, Fughhi IAM, Ng R, Chukkapalli V, Shah P, et al. Impact of cachexia on outcomes in aggressive lymphomas. Ann Hematol. 2017;96:951–6. https://doi.org/10.1007/s00277-017-2958-1.
5. Petruzzelli M, Schweiger M, Schreiber R, Campos-Olivas R, Tsoli M, Allen J, et al. A switch from White to Brown Fat increases Energy Expenditure in Cancer-Associated Cachexia. Cell Metab. 2014;20:433–47. https://doi.org/10.1016/j.cmet.2014.06.011.
6. Jin J, Miao C, Wang Z, Zhang W, Zhang X, Xie X, et al. Design and synthesis of aryloxypropanolamine as β3-adrenergic receptor antagonist in cancer and lipolysis. Eur J Med Chem. 2018;150:757–70. https://doi.org/10.1016/j.ejmech.2018.03.032.

7. Qiao G, Chen M, Bucsek MJ, Repasky EA, Hylander BL. Adrenergic signaling: a targetable checkpoint limiting development of the Antitumor Immune Response. Front Immunol 2018;9. https://doi.org/10.3389/fimmu.2018.00164
8. Caballero-Hernandez D, Najera-Valderrabano D, Valadez-Lira A, Franco-Molina M, Gomez-Flores R, Tamez-Guerra P, et al. Alterations of antitumor and metabolic responses in L5178Y-R lymphoma-bearing mice after only 30-minute daily chronic stress exposure. Exp Oncol. 2017;39:276–80.
9. Burkart M, Schieber M, Basu S, Shah P, Venugopal P, Borgia JA, et al. Evaluation of the impact of cachexia on clinical outcomes in aggressive lymphoma. Br J Haematol. 2019;186:45–53. https://doi.org/10.1111/bjh.15889.
10. Długosz-Danecka M, Gruszka AM, Szmit S, Olszanecka A, Ogórka T, Sobociński M, et al. Primary cardioprotection reduces mortality in Lymphoma patients with increased risk of Anthracycline Cardiotoxicity, treated by R-CHOP regimen. Chemotherapy. 2018;63:238–45. https://doi.org/10.1159/000492942.
11. Cao Y. Adipocyte and lipid metabolism in cancer drug resistance. J Clin Invest. 2019;129:3006–17. https://doi.org/10.1172/JCI127201.
12. Bilora F, Veronese F, Zancan A, Biasiolo M, Pomerri F, Muzzio PC. Autonomic dysfunction in Hodgkin and non-hodgkin lymphoma. A paraneoplastic syndrome? Hematol Rep. 2010;2:e8. https://doi.org/10.4081/hr.2010.e8.
13. Wu H-F, Yu W, Saito-Diaz K, Huang C-W, Carey J, Lefcort F, et al. Norepinephrine transporter defects lead to sympathetic hyperactivity in familial dysautonomia models. Nat Commun. 2022;13:7032. https://doi.org/10.1038/s41467-022-34811-7.
14. Straka T, Vita V, Prokshi K, Hörner SJ, Khan MM, Pirazzini M, et al. Postnatal Development and Distribution of Sympathetic Innervation in mouse skeletal muscle. Int J Mol Sci. 2018;19. https://doi.org/10.3390/ijms19071935.
15. Horvathova L, Tillinger A, Padova A, Mravec B. Sympathectomized tumor-bearing mice survive longer but develop bigger melanomas. Endocr Regul. 2016;50:207–14. https://doi.org/10.1515/enr-2016-0022.
16. Friedman JM, Leibel RL, Siegel DS, Walsh J, Bahary N. Molecular mapping of the mouse ob mutation. Genomics. 1991;11:1054–62. https://doi.org/10.1016/0888-7543(91)90032-A.
17. Livak KJ, Schmittgen TD. Analysis of relative gene expression data using real-time quantitative PCR and the 2 – ΔΔCT. Method Methods. 2001;25:402–8. https://doi.org/10.1006/meth.2001.1262.
18. Galarraga M, Campión J, Muñoz-Barrutia A, Boqué N, Moreno H, Martínez JA, et al. Adiposoft: automated software for the analysis of white adipose tissue cellularity in histological sections. J Lipid Res. 2012;53:2791–6. https://doi.org/10.1194/jlr.D023788.
19. Collins S. β-Adrenergic receptors and adipose tissue metabolism: evolution of an Old Story. Annu Rev Physiol. 2022;84:1–16. https://doi.org/10.1146/annurev-physiol-060721-092939.
20. Hylander BL, Repasky EA. Thermoneutrality, mice, and Cancer: a heated opinion. Trends Cancer. 2016;2:166–75. https://doi.org/10.1016/j.trecan.2016.03.005.
21. Tabuchi C, Sul HS. Signaling pathways regulating thermogenesis. Front Endocrinol (Lausanne). 2021;12. https://doi.org/10.3389/fendo.2021.595020.
22. Han J, Meng Q, Shen L, Wu G. Interleukin-6 induces fat loss in cancer cachexia by promoting white adipose tissue lipolysis and browning. Lipids Health Dis. 2018;17:14. https://doi.org/10.1186/s12944-018-0657-0.
23. Chun K-H. Mouse model of the adipose organ: the heterogeneous anatomical characteristics. Arch Pharm Res. 2021;44:857–75. https://doi.org/10.1007/s12272-021-01350-6.
24. Paval DR, Patton R, McDonald J, Skipworth RJE, Gallagher IJ, Laird BJ. A systematic review examining the relationship between cytokines and cachexia in incurable cancer. J Cachexia Sarcopenia Muscle. 2022;13:824–38. https://doi.org/10.1002/jcsm.12912.
25. Chiappalupi S, Sorci G, Vukasinovic A, Salvadori L, Sagheddu R, Coletti D, et al. Targeting RAGE prevents muscle wasting and prolongs survival in cancer cachexia. J Cachexia Sarcopenia Muscle. 2020;11:929–46. https://doi.org/10.1002/jcsm.12561.
26. Yamashita AS, das Neves RX, Rosa-Neto JC, Lira F, dos S, Batista ML, Alcantara PS, et al. White adipose tissue IFN-γ expression and signalling along the progression of rodent cancer cachexia. Cytokine. 2017;89:122–6. https://doi.org/10.1016/j.cyto.2016.02.015.
27. Pototschnig I, Feiler U, Diwoky C, Vesely PW, Rauchenwald T, Paar M, et al. Interleukin-6 initiates muscle- and adipose tissue wasting in a novel C57BL/6 model of cancer-associated cachexia. J Cachexia Sarcopenia Muscle. 2023;14:93–107. https://doi.org/10.1002/jcsm.13109.
28. Dwarkasing JT, Witkamp RF, Boekschoten MV, Ter Laak MC, Heins MS, van Norren K. Increased hypothalamic serotonin turnover in inflammation-induced anorexia. BMC Neurosci. 2016;17:26. https://doi.org/10.1186/s12868-016-0260-0.
29. Richard JE, López-Ferreras L, Chanclón B, Eerola K, Micallef P, Skibicka KP, et al. CNS β_3 -adrenergic receptor activation regulates feeding behavior, white fat browning, and body weight. Am J Physiology-Endocrinology Metabolism. 2017;313:E344–58. https://doi.org/10.1152/ajpendo.00418.2016.
30. Nissen MD, Sloan EK, Mattarollo SR. β-Adrenergic signaling impairs Antitumor CD8 + T-cell responses to B-cell Lymphoma Immunotherapy. Cancer Immunol Res. 2018;6:98–109. https://doi.org/10.1158/2326-6066.CIR-17-0401.
31. Mustafa S, Koran S, AlOmair L. Insights into the role of Matrix metalloproteinases in Cancer and its various therapeutic aspects: a review. Front Mol Biosci. 2022;9. https://doi.org/10.3389/fmolb.2022.896099.
32. Barbieri A, Bimonte S, Palma G, Luciano A, Rea D, Giudice A, et al. The stress hormone norepinephrine increases migration of prostate cancer cells in vitro and in vivo. Int J Oncol. 2015;47:527–34. https://doi.org/10.3892/ijo.2015.3038.
33. Devine RD, Bicer S, Reiser PJ, Velten M, Wold LE. Metalloproteinase expression is altered in cardiac and skeletal muscle in cancer cachexia. Am J Physiol Heart Circul Physiol. 2015;309(4):H685——91. https://doi.org/10.1152/ajpheart.00106.2015.

Publisher's note